## Short Communication

# Vertically Aligned CuO Nanowires Based Electrode for Amperometric Detection of Hydrogen Peroxide

*Wenzhao Jia,*[a] *Min Guo,*[b] *Zhe Zheng,*[c] *Ting Yu,*[c] *Ying Wang,*[a] *Edgar G. Rodriguez,*[a] *Yu Lei*[a]*

[a]  Department of Chemical, Materials and Biomolecular Engineering, University of Connecticut, 191 Auditorium Road, Unit 3222, Storrs, CT 06269-3222, USA
*e-mail: ylei@engr.uconn.edu
[b]  School of Electrical and Electronic Engineering, Nanyang Technological University, Singapore 637371, Singapore
[c]  School of Physical and Mathematical Sciences, Nanyang Technological University, Singapore 637371, Singapore

### Abstract

Vertically aligned copper oxide (CuO) nanowires were synthesized by directly heating copper foil on a hotplate under ambient conditions. The as-grown CuO nanowires film is mechanically stable and was facilely attached to a glassy carbon (GC) electrode, offering an excellent electrochemical sensing platform. The CuO nanowires electrode shows excellent electrocatalytic response to $H_2O_2$ with significantly lower overpotentials for its oxidation and reduction and also exhibits a fast response and high sensitivity for the amperometric detection of $H_2O_2$. The novel vertically aligned CuO nanowires electrode is readily applicable to other analytes and has great potential applications in the electrochemical detection.

**Keywords:** CuO, Nanowires, Reduction, Oxidation, Hydrogen peroxide

Hydrogen peroxide ($H_2O_2$), a strong oxidant, has been widely used in many fields, including food production [1–3], pulp and paper bleaching [4, 5], sterilization [6], the oxidation of organic substances [7–9], liquid-based fuel cells [10–14], and clinical applications [15, 16]. $H_2O_2$ is also readily present in a variety of commercial products such as cosmetic and pharmaceutical products [17]. Furthermore, as a product of enzymatic reactions catalyzed by a large number of oxidases, $H_2O_2$ concentration can be correlated to the concentration of target substrates, thus is practically important in the field of biosensor development [18–22]. Consequently, there are growing interests to study the oxidation and reduction of $H_2O_2$ at different electrode surfaces, and the detection and quantification of $H_2O_2$ still remains a significant endeavor in various fields.

In the past decades, many analytical methods, such as titration [23], spectrophotometric [24, 25], fluorometric [26, 27], chemiluminescence [28, 29], and chromatographic [30–32] techniques have been developed for the detection and quantification of $H_2O_2$. Although sensitive and reliable, these methods are either time-consuming or expensive, and/or require skilled personnel, therefore they are unsuitable for rapid and cost-effective determination of $H_2O_2$. Thus, electrochemical methods have emerged as a preferable alternative, owing to their relatively low cost, efficiency, high sensitivity, and ease of operation [33–41]. With the development of nanotechnology, new efforts have been emphasized on using novel nanomaterials to reduce the overpotentials for $H_2O_2$ oxidation and reduction and

minimize the interference. CuO, a p-type semiconductor with a narrow band gap of 1.2 eV, is promising in such application because CuO nanostructures have unique advantages including the high specific surface area, chemical stability, electrochemical activity, and high electron communication features. Recently CuO nanoparticles were immobilized on a Nafion membrane coated platinum electrode and proved to perform well as $H_2O_2$ reduction catalysts in a strong basic solution (0.1 M NaOH) as CuO nanoparticles play an important role in transferring electrons between $H_2O_2$ and an electrode as well as enabling regeneration after electron exchanges with $H_2O_2$ [34]. However, the nanoparticles can not stand alone and require a matrix to entrap them for electrode attachment. The major disadvantages of entrapment of CuO nanoparticles are the strong diffusion resistance offered by the entrapment material and the limited accessibility of the nanoparticles to analytes. Meanwhile, the use of strong basic solution in the reduction of $H_2O_2$ potentially limits its further application in biosensors because most of biomolecules can not survive in such harsh condition. Therefore, there remains a need for simpler processes to fabricate novel CuO nanomaterials with superior catalytic property for fast, sensitive, reliable, and stable detection of $H_2O_2$. Preferably, the novel CuO nanomaterials are free-standing, have excellent mechanical and electrocatalytic properties, and can be easily manipulated and attached to the electrode surface without the help of an entrapment matrix.
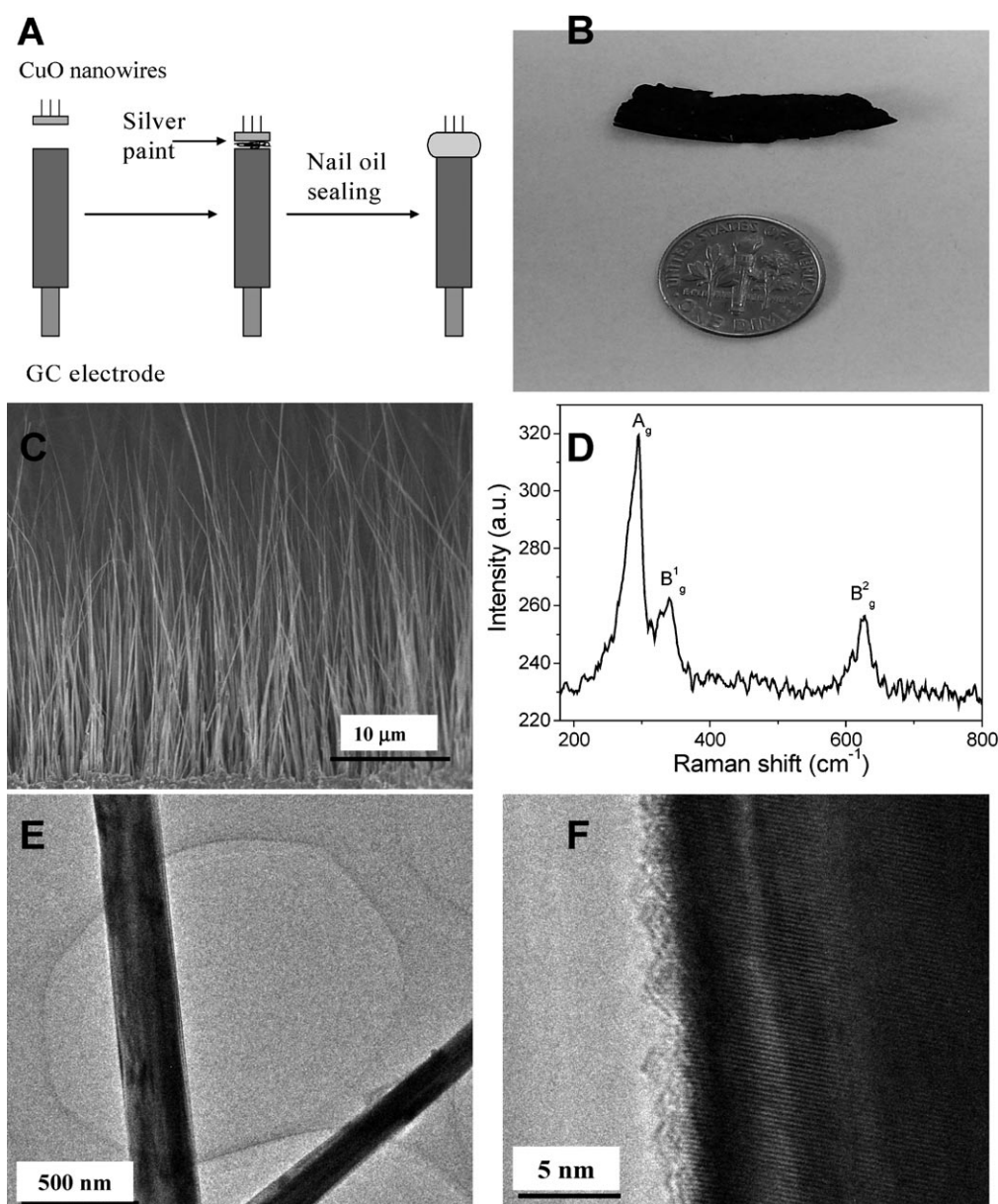
Fig. 1.    A) A schematic of the fabrication of CuO nanowires electrode. B) Optical image of as-grown CuO nanowires film. C) SEM image of vertically aligned CuO nanowires. D) Micro-Raman spectrum of the CuO nanowires. E) Typical TEM image of the CuO nanowires. F) HRTEM image of a CuO nanowire.

In this article, we reported the synthesis of vertically aligned CuO nanowires film, the fabrication of CuO nanowires electrode, and its application in the electrocatalytic oxidation and reduction of $H_2O_2$ in 0.01 M pH 7.4 phosphate buffer solution. The vertically aligned CuO nanowires electrode was also served as an electrochemical sensing platform for the sensitive amperometric detection of $H_2O_2$. Compared to traditional electrodes, the as-prepared CuO nanowires electrode has great surface area, a minimized mass-transport resistance, high surface energy, and enhanced electron transfer, leading to electrocatalytic oxidation and reduction of $H_2O_2$ at lower overpotentials. The results also demonstrate the CuO nanowires electrode has

great potential applications in sensor and biosensor development.

Figures 1A and 1B show a schematic of the electrode fabrication and an optical image of the as-prepared CuO nanowires film, respectively. The size of vertically aligned CuO nanowire film is solely dependent on the size of copper foil used. The synthesized CuO nanowires film is freestanding and can be manipulated using tweezers with carefulness. The typical morphology of the as-prepared CuO nanowires film is presented in Figure 1C. One can see that the surface is fully covered with a large amount of vertically aligned nanowire-like morphologies. The diameters of the nanowires vary from about 20 nm to 150 nm and

the lengths are several tens of micrometers. Fig. 1D displays a typical Raman spectrum for the sample collected from the surface layer. Three peaks corresponding to $A_g$ (296 cm$^{-1}$), $B_g^{(1)}$ (346 cm$^{-1}$), and $B_g^{(2)}$ (636 cm$^{-1}$) modes of bulk CuO crystals, respectively, were observed, indicating the surface layer is fully covered by CuO. The detailed structure of an individual CuO nanowire is studied by TEM and HRTEM. As shown in Figures 1E and 1F, CuO nanowire formed has a single crystal property. The spacing of the lattice planes 0.235 nm corresponds to the interspacing of (111) plane in monoclinic CuO.

In order to evaluate the electrocatalytic property of the as-prepared CuO nanowires, the cyclic voltammogram (CV) was carried out to study $H_2O_2$ oxidation and reduction. $H_2O_2$ was selected as a model compound in this study because the oxidation and reduction of $H_2O_2$ are practically important in the fields of biosensor and fuel cell development [3]. Figure 2 shows the CVs of CuO nanowires electrode and a bare GC electrode in the absence and presence of 10 mM $H_2O_2$ at pH 7.4 phosphate buffer solution. As shown for a bare GC electrode, there is only a small background current observed in buffer, while a dramatic increase of current signal toward the positive and negative ends of the potential range was observed when CuO nanowires electrode was used in buffer, which may be attributed to the large surface area, high surface energy, and enhanced electron transfer of as-synthesized CuO nanowires. Upon the addition of 10 mM $H_2O_2$, one can see no obvious redox response to $H_2O_2$ is observed over most of the potential range at a bare GC electrode. However, at CuO nanowires electrode, both oxidation and reduction currents were greatly enhanced due to the strong electrocatalytic reaction of $H_2O_2$. The oxidation and reduction processes start at ca. $+0.4$ V and $+0.05$ V (vs. Ag/AgCl), respectively. Compared to the bare GC electrode, CuO nanowires electrode offers a marked decrease in the overvoltages for $H_2O_2$ oxidation and reduction, which allows convenient low-potential amperometric detection. These results demonstrate that CuO nanowires have excellent electrocatalytical ability and the enhanced response may be attributed to many transport channels in nanoscale provided by CuO nanowires, excellent accessibility of CuO nanowires to analytes, as well as enhanced electron transfer reaction between $H_2O_2$ and CuO nanowires.

The superior electrocatalytic ability and easy manipulation makes the as-prepared vertically aligned CuO nanowires promising in the detection of $H_2O_2$. As the CVs indicated that $H_2O_2$ can be strongly oxidized and reduced at the CuO nanowires electrode, the amperometric detection of $H_2O_2$ based on oxidation and reduction current was demonstrated at applied potentials of $+0.6$ V and $-0.2$ V, respectively. Figure 3A shows typical amperometric responses (steady-state current vs. time) of the CuO nanowires electrode to the successive additions of $H_2O_2$ at an applied potential of $+0.6$ V. The CuO nanowires electrode responds rapidly to the changes in $H_2O_2$ concentration, producing steady-state signals within 5 s. The corresponding calibration curve is presented in Figure 3B. The plot was
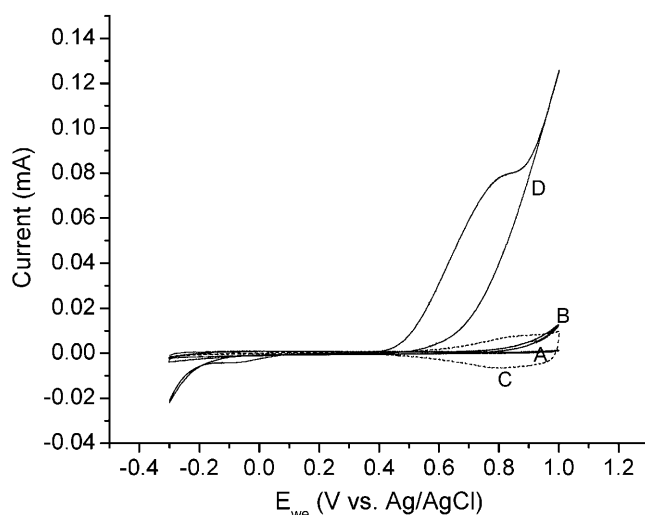


Fig. 2. Cyclic voltammograms of the CuO nanowires electrode and a bare glassy carbon (GC) electrode in 0.01 M pH 7.4 phosphate buffer in the absence and presence of 10 mM $H_2O_2$, respectively. Scan rate = 50 mV/s. A) GC electrode in buffer. B) GC electrode in 10 mM $H_2O_2$. C) CuO nanowires electrode in buffer. D) CuO nanowires electrode in 10 mM $H_2O_2$.

linear up to 1.68 mM with a sensitivity of 204.15 μA cm$^{-2}$ mM$^{-1}$ ($R = 0.9884$), while for a higher concentration of $H_2O_2$, the plot deviates from linearity, which may be attributed to the saturation of the electrocatalytic activity of CuO nanowires. The sensitivity and fast response of CuO nanowires electrode to $H_2O_2$ are impressive at the applied potential of $+0.6$ V, however, some electroactive compounds can be oxidized at this applied potential and may potentially interfere the detection of $H_2O_2$. It has been reported the amperometric response at an applied potential of $+0.4$ V is overlapped by large anodic contributions from compounds such as ascorbic acid, uric acid, and acetaminophen, whereas no interference was observed at a potential of $-0.2$ V for these compounds [42]. In order to minimize the biases from the potential interferences presented in the real samples, the possibility to perform amperometric detection of $H_2O_2$ based on the reduction was also investigated. Figure 3C shows the amperometric response of the CuO nanowires electrode to the successive injections of $H_2O_2$ at an applied potential of $-0.2$ V. The corresponding calibration curve is presented in Figure 3D. An applied potential of $-0.2$ V was chosen because the interference from oxygen reduction can be eliminated [42]. As shown in the figure, well-defined responses were obtained for the successive additions of 10 μM, 50 μM, 100 μM, 500 μM, and 1 mM of $H_2O_2$, respectively. The catalytic reduction of $H_2O_2$ at the surface of CuO nanowires is very fast in reaching a dynamic equilibrium upon each addition of $H_2O_2$, generating a steady-state current signal within 5 s. These results demonstrate a stable and efficient catalytic property of CuO nanowires. The response of the CuO nanowires electrode to $H_2O_2$ is linear up to 28.87 mM with a sensitivity of 30.11 μA cm$^{-2}$ mM$^{-1}$ ($R = 0.9996$) and also saturated at a higher concentration. The most appealing aspect for the detection
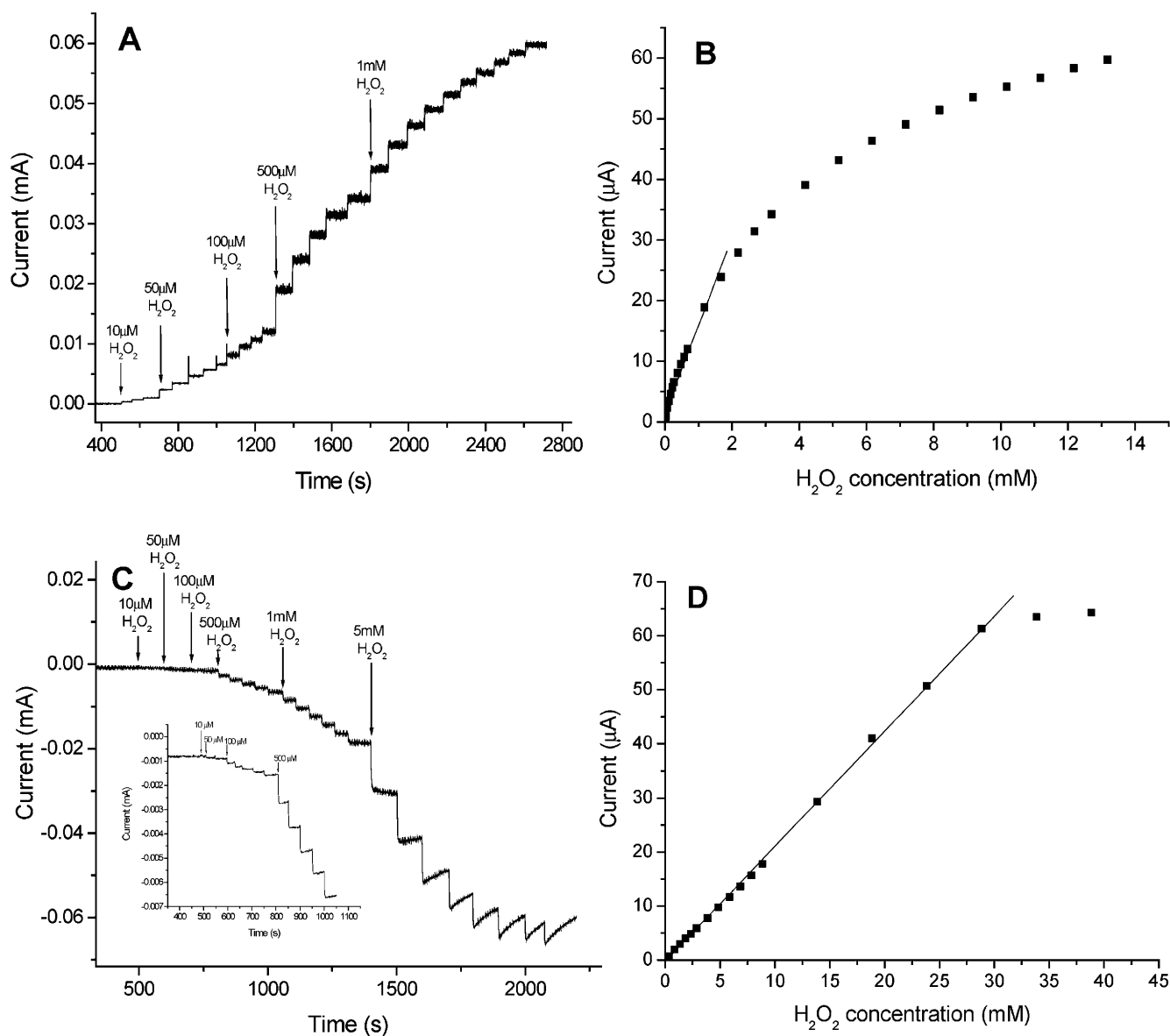
Fig. 3.   Amperometric response of CuO nanowires electrode with successive additions of $H_2O_2$ to 0.01 M pH 7.4 phosphate buffer. A) $i-t$ response at an applied potential of $+0.6$ V (vs. Ag/AgCl) and B) its corresponding calibration plot. C) $i-t$ response at an applied potential of $-0.2$ V (vs. Ag/AgCl) and D) its corresponding calibration plot.

of $H_2O_2$ at $-0.2$ V is that a lot of interferences can be substantially eliminated and more selective analysis of $H_2O_2$ can be achieved. In addition, it can potentially eliminate the need for permselective membrane barriers or artificial electron mediators, thus greatly simplifying the sensor fabrication and enhancing the sensor performance.

In conclusion, we have demonstrated the synthesis of single crystal and vertically aligned CuO nanowires film and its application for the fast and sensitive detection of $H_2O_2$. The as-prepared vertically aligned CuO nanowires possess high specific surface area and directly expose to the environment, allowing the free access of analytes to CuO surface. Moreover, the single crystalline CuO nanowires have good conductivity, which provide many transport channels in nanoscale, and thus, enhancing the electron

transfer reaction between $H_2O_2$ and CuO. All these features provide a favorable environment for the electrocatalytic oxidation and reduction of $H_2O_2$ and allow the sensitive detection of $H_2O_2$ at both positive and negative applied potentials at physiological pH. The novel CuO nanowires electrode demonstrated in this study shows great potential applications in sensor and biosensor development.

## Experimental

The vertically aligned CuO nanowire film was prepared by a simple hot-plate method under ambient conditions [43, 44]. Briefly, a copper foil (Sigma-Aldrich) was used as both substrate and starting material. After being polished and cleaned, the copper foil was heated on a hot-plate at 400 °C

for 10 hours in air. After cooling to the room temperature, a black layer was formed on the copper plate. The black top layer was peeled off carefully and its morphology was investigated by scanning electron microscopy, high-resolution transmission electron microscopy, and micro-Raman spectroscopy. To fabricate the electrode, the vertically aligned CuO nanowires grown on the copper plate with an appropriate size was attached to the surface of a glassy carbon (GC) electrode using conductive silver paint. In order to prevent the exposure of silver paint to the solution, nail enamel was used to insulate the edge of substrate and GC electrode. Therefore, only the CuO nanowires were exposed to the environment and the exposure area had the same diameter (3 mm) as that of a GC electrode. Cyclic voltammetric (CV) and amperometric experiments were performed using an electrochemical workstation (Bio-logic SA VMP2) coupled to a computer. All experiments were conducted using a three-electrode electrochemical cell (10-mL volume with a working volume of 5 mL), with a working electrode (CuO nanowires electrode or a bare GC electrode), an Ag/AgCl reference electrode (MF-2079, BAS), and a platinum wire auxiliary electrode. $H_2O_2$ measurement was carried out in 0.01 M pH 7.4 phosphate buffer at room temperature. For CV measurements, the potential was scanned from $-0.3$ V to 1.0 V with a scan rate of 50 mV/s. For amperometric detection, all measurements were performed by applying an appropriate potential (vs. Ag/AgCl) to the working electrode and allowing the transient background current to decay to a steady-state value, prior to the addition of $H_2O_2$. The current response due to the addition of $H_2O_2$ was recorded. A stirred solution was employed to provide convective transport.

## References

[1] H. Elzanowska, E. Abu-Irhayem, B. Skrzynecka, V. I. Birss, *Electroanalysis* **2004**, *16*, 478.
[2] F. M. Jin, A. Kishita, T. Moriya, H. Enomoto, *J. Supercrit. Fluid* **2001**, *19*, 251.
[3] A. Salimi, R. Hallaj, S. Soltanian, H. Mamkhezri, *Anal. Chim. Acta* **2007**, *594*, 24.
[4] M. C. Depew, T. Antimirova, Y. G. Chen, J. K. S. Wan, *Res. Chem. Intermediat.* **1999**, *25*, 497.
[5] E. C. Xu, *J. Pulp Pap. Sci.* **2002**, *28*, 379.
[6] M. Yamamoto, M. Nishioka, M. Sadakata, *J. Electrostat.* **2002**, *55*, 173.
[7] Y. P. Huang, J. Li, W. H. Ma, M. M. Cheng, J. C. Zhao, J. C. Yu, *J. Phys. Chem. B* **2004**, *108*, 7263.
[8] S. R. Sarathy, M. Mohseni, *Environ. Sci. Technol.* **2007**, *41*, 8315.
[9] Y. Usui, K. Sato, M. Tanaka, *Angew. Chem. Int. Ed.* **2003**, *42*, 5623.
[10] N. A. Choudhury, R. K. Raman, S. Sampath, A. K. Shukla, *J. Power Sources* **2005**, *143*, 1.
[11] E. Kjeang, A. G. Brolo, D. A. Harrington, N. Djilali, D. Sinton, *J. Electrochem. Soc.* **2007**, *154*, B1220.
[12] G. H. Miley, N. Luo, J. Mather, R. Burton, G. Hawkins, L. F. Gu, E. Byrd, R. Gimlin, P. J. Shrestha, G. Benavides, J. Laystrom, D. Carroll, *J. Power Sources* **2007**, *165*, 509.
[13] R. K. Raman, A. K. Shukla, *Fuel Cells* **2007**, *7*, 225.
[14] A. Ramanavicius, A. Kausaite, A. Ramanaviciene, *Biosens. Bioelectron.* **2005**, *20*, 1962.
[15] M. Rosin, A. Kramer, M. Hanschke, *J. Dent. Res.* **1997**, *76*, 291.
[16] E. Swift, H. Heymann, A. Wilder, A. St-Georges, M. Nunes, *J. Dent. Res.* **2002**, *81*, A253.
[17] L. Campanella, R. Roversi, M. P. Sammartino, M. Tomassetti, *J. Pharm. Biomed. Anal.* **1998**, *18*, 105.
[18] S. Cosnier, S. Szunerits, R. S. Marks, A. Novoa, L. Puech, E. Perez, I. Rico-Lattes, *Electrochem. Commun.* **2000**, *2*, 851.
[19] M. D. Gouda, M. A. Kumar, M. S. Thakur, N. G. Karanth, *Biosens. Bioelectron.* **2002**, *17*, 503.
[20] J. X. Wang, X. W. Sun, A. Wei, Y. Lei, X. P. Cai, C. M. Li, Z. L. Dong, *Appl. Phys. Lett.* **2006**, *88*, 233106.
[21] A. Wei, X. W. Sun, J. X. Wang, Y. Lei, X. P. Cai, C. M. Li, Z. L. Dong, W. Huang, *Appl. Phys. Lett.* **2006**, *89*, 123902.
[22] Y. J. Zou, C. L. Xiang, L. X. Sun, F. Xu, *Biosens. Bioelectron.* **2008**, *23*, 1010.
[23] N. V. Klassen, D. Marchington, H. C. E. Mcgowan, *Anal. Chem.* **1994**, *66*, 2921.
[24] R. C. Matos, E. O. Coelho, C. F. de Souza, F. A. Guedes, M. A. Matos, *Talanta* **2006**, *69*, 1208.
[25] P. A. Tanner, A. Y. S. Wong, *Anal. Chim. Acta* **1998**, *370*, 279.
[26] I. Mori, K. Takasaki, Y. Fujita, T. Matsuo, *Talanta* **1998**, *47*, 631.
[27] A. Sakuragawa, T. Taniai, T. Okutani, *Anal. Chim. Acta* **1998**, *374*, 191.
[28] G. M. Greenway, T. Leelasattarathkul, S. Liawruangrath, R. A. Wheatley, N. Youngvises, *Analyst* **2006**, *131*, 501.
[29] J. C. Yuan, A. M. Shiller, *Anal. Chem.* **1999**, *71*, 1975.
[30] T. H. Huang, M. E. Garceau, P. Gao, *J. Pharm. Biomed. Anal.* **2003**, *31*, 1203.
[31] S. Oszwaldowski, R. Lipka, M. Jarosz, *Anal. Chim. Acta* **2000**, *421*, 35.
[32] U. Pinkernell, S. Effkemann, U. Karst, *Anal. Chem.* **1997**, *69*, 3623.
[33] T. A. Ivandini, R. Sato, Y. Makide, A. Fujishima, Y. Einaga, *Diamond Relat. Mater.* **2005**, *14*, 2133.
[34] X. M. Miao, R. Yuan, Y. Q. Chai, Y. T. Shi, Y. Y. Yuan, *J. Electroanal. Chem.* **2006**, *612*, 157.
[35] L. Muresan, G. L. Turdean, I. C. Popescu, *J. Appl. Electrochem.* **2008**, *38*, 349.
[36] P. Santhosh, K. M. Manesh, A. Gopalan, K. P. Lee, *Anal. Chim. Acta* **2006**, *575*, 32.
[37] Y. Shen, M. Trauble, G. Wittstock, *Anal. Chem.* **2008**, *80*, 750.
[38] Q. F. Sheng, H. Yu, H. B. Zheng, *Electrochim. Acta* **2007**, *52*, 7300.
[39] K. Thenmozhi, S. S. Narayanan, *Sens. Actuators B, Chem.* **2007**, *125*, 195.
[40] S. G. Wu, T. L. Wang, C. Q. Wang, Z. Y. Gao, C. Q. Wang, *Electroanalysis* **2007**, *19*, 659.
[41] Y. J. Zou, L. X. Sun, F. Xu, *Talanta* **2007**, *72*, 437.
[42] Y. H. Lin, F. Lu, Y. Tu, Z. F. Ren, *Nano Lett.* **2004**, *4*, 191.
[43] T. Yu, X. Zhao, Z. X. Shen, Y. H. Wu, W. H. Su, *J. Cryst. Growth* **2004**, *268*, 590.
[44] Y. W. Zhu, A. M. Moo, T. Yu, X. J. Xu, X. Y. Gao, Y. J. Liu, C. T. Lim, Z. X. Shen, C. K. Ong, A. T. S. Wee, J. T. L. Thong, C. H. Sow, *Chem. Phys. Lett.* **2006**, *419*, 458.